ISBN 978-83-927084-8-3
ISSN 0867-7964

HYSTERESIS EFFECTS IN SPLASH SEDIMENT TRANSPORT

Mohsen Cheraghi [a], Seifeddine Jomaa [b], Graham C. Sander [c], D. A. Barry [a]

[a] *Laboratoire de technologie écologique, Institut d'ingénierie de l'environnement, Faculté de l'environnement naturel, architectural et construit (ENAC), Station 2, Ecole Polytechnique Fédérale de Lausanne (EPFL), 1015 Lausanne, Switzerland*
E-mails addresses: mohsen.cheraghi@epfl.ch, andrew.barry@epfl.ch

[b] *Department of Aquatic Ecosystem Analysis and Management, Helmholtz Centre for Environmental Research – UFZ, Brueckstrasse 3a, 39114 Magdeburg, Germany.*
E-mail address: seifeddine.jomaa@ufz.de

[c] *Department of Civil and Building Engineering, Loughborough University, Loughborough LE11 3TU United Kingdom.*
E-mail address: g.sander@lboro.ac.uk

Abstract: Temporally variable rainfall was applied on an initially dry, ploughed and smoothed agricultural soil to investigate the hysteresis pattern in the sediment concentration-discharge relation using laboratory flume experiments. The erosion flume had dimensions of 5-m × 2-m and consisted of two collectors at either side of the outlet. The slope was fixed at 2% and a sequence of seven events involving 20-min precipitation (rates of 15, 30, 45, 60, 45, 30 and 15 mm h^{-1}) were imposed. Due to the cohesive agricultural soil, low discharge and slope, rainfall detachment was the only erosion mechanism operating. The data collected at the two flume exits were analysed by measuring the discharge and total sediment concentration. A clockwise hysteresis loop was found for total sediment concentration because of the easily erodible soil condition at the beginning of the experiment. It was also found that the Hairsine-Rose (HR) model was in agreement with the experimental data, which showed its capability to predict the characteristics of hysteretic sediment transport arising in time varying rainfall events.

KEY WORDS: Hysteresis effects, Sediment transport, Flume experiment, Splash soil erosion, Hairsine and Rose model.

1. INTRODUCTION

Transport of sediment within and from catchments has important environmental and ecological implications. Over the years many studies were carried out on sediment transport in rivers (Walling and Webb, 1985; Batalla et al., 2004; Halliday et al., 2014). These showed that sediment fluxes, or concentration, are different on the rising as opposed to falling limb of river discharge. Different types of loops – termed hysteresis loops – appear in the discharge-sediment concentration relationship. Motivated by this, we hypothesise that hysteresis loops appear also in sediment transport in shallow

overland flow, e.g., precipitation-driven erosion, and report a laboratory experiment designed to capture this behaviour.

Among different process-based soil erosion models applicable to precipitation-driven erosion, the HR model has been shown to explain soil erosion of both the different particle size contributions and the total suspended sediment. Numerous experimental (Gao et al., 2003; Heilig et al., 2001; Jomaa et al., 2013, 2012) and theoretical (Barry et al., 2010; Hairsine et al., 1999; Kinnell, 2013; Lisle et al., 1998; Parlange et al., 1999; Sander et al., 1996) investigations have been carried out to validate and analyse the model.

Sander et al. (2011) reported a theoretical study on this model where they showed it predict different hysteresis loops (in sediment concentration versus discharge plots) for entrainment and detachment-driven erosion. They also validated the model against the hysteretic experimental results of Polyakov & Nearing (2003) for flow-driven erosion. Thus, in this study the main objective was to further validate the model's predictions of hysteresis using temporally varying rainfall rates and for which raindrop detachment was the dominant erosive mechanism.

2. EXPERIMENTAL SETUP

The setup of the EPFL erosion flume is shown in Figure 1. Rainfall with uniformity coefficient of 0.85 (Jomaa et al., 2010; Tromp-van Meerveld et al., 2008) was generated using 10 sprinklers on two oscillating bars 3 m above the soil surface. Water was ejected from the sprinklers with a pressure of 1.2 bar, while the precipitation rate was controlled via changing the oscillation frequency. There were two collectors at the downstream end that sampled the transported sediment. A more detailed description of the flume is provided in Baril (1991), Jomaa et al. (2010) and Viani (1986). The agricultural soil in the flume was taken from Sullens (Vaud), Switzerland, and prior to the start of the rainfall the soil surface was ploughed to a depth of 20 cm and smoothed as outlined in Jomaa et al. (2010).

The soil was subdivided into seven different particle sizes classes (< 2, 2-20, 20-50, 50-100, 100-315, 315-1000 and > 1000 μm) from which the corresponding mass proportions and settling velocities for the HR model were obtained (Jomaa et al., 2010, 2012, 2013). In our experiment, the stream power was estimated as 0.013 W m^{-2}, which is below the critical value of 0.15-0.20 W m^{-2} (Beuselinck et al., 2002) required for flow-driven entrainment. Therefore, the sediment eroded and transported was due to raindrop impact.

As shown in Figure 2, seven sequential rainfall events of 20-min duration with intensities of 15, 30, 45, 60, 45, 30 and 15 mm h^{-1} were imposed. The increasing sequence of rainfall rates from 15 → 60 mm hr^{-1} are denoted E1 - E4 and the decreasing sequence of 45 → 15 mm hr^{-1} are labelled as E5 - E7. All runoff was collected continuously at the flume outlets for the first 10 mins of the experiment, after which samples were collected every 3 mins.

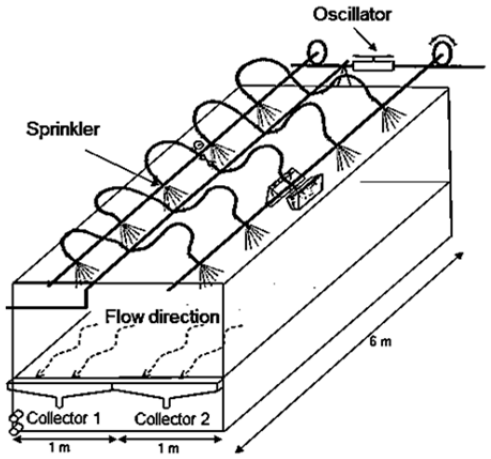

Figure 1. Outline of the EPFL erosion flume. The size of the flume is 5-m × 2-m and the precipitation rate can be adjusted based on the oscillation frequency of the sprinklers.

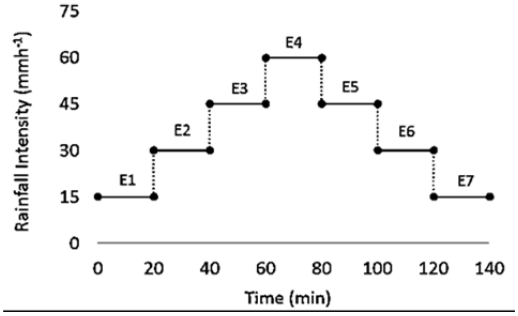

Figure 2. Temporal variation in the precipitation rate, which consisted of seven rainfall events (no pauses).

3. MODEL

The governing equations and underlying assumptions of the HR model are provided elsewhere (Barry et al., 2010; Hairsine and Rose, 1992, 1991; Sander et al., 1996). The fundamental difference between the HR approach and other erosion models is that it considers eroded sediment to be either in suspension or at the soil surface, where it forms a deposited layer of low-cohesion sediment. The key model parameters are the detachability (inversely proportional to soil cohesion) of the uneroded soil (a), the redetachability of the deposited soil (a_d), the critical mass per unit area of the deposited layer (m^*) and the overland flow water depth (D). The parameter m^* is the amount of the deposited soil to completely protect the original soil from further erosion. All parameters reported below were obtained by fitting the model using the Particle Swarm Optimization method (PSO).

4. RESULTS AND DISCUSSION

4.1. DISCHARGE

The time variation of discharge during the experiment is shown in Figure 3. As the soil surface was initially dry, the transient effects of infiltration are clearly evident during the first two rainfall periods, as steady-state discharge was not achieved until after 30 min. By this time the upper soil profile had become saturated, and steady-state discharge was quickly achieved in all subsequent periods following the change in rainfall intensity. Differences in discharges between collectors 1 and 2 indicate that overland flow was not fully one-dimensional.

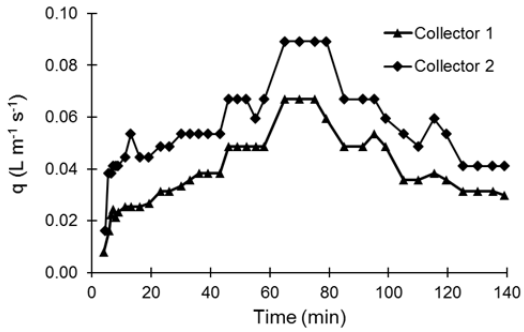

Figure 3. The observed discharge of the collectors 1 and 2. The flow rate of collector 2 is greater than collector 1 due to the two-dimensional nature of the flow on the soil surface.

4.2. TOTAL SEDIMENT CONCENTRATION

Figure 4 shows an early rise in the concentration as a result of the rapid injection of sediment from raindrop detachment at the start of the experiment. This was followed by a rapid decline due to removal of easily erodible sediment from suspension, as well as the development of a layer of deposited sediment. The deposited layer composition was dominated by larger particles due to gravity settlement. The erosion of the smaller particles from the original (non-eroded) soil, which is responsible for the peak concentration, was then significantly reduced and the concentration declines. The magnitude of the initial peak is governed by both the rainfall rate and the detachability of the soil at $t = 0$. This process was then repeated for the next three increasing rainfall periods, i.e., we see a peak occurring at the start of each successive period followed by a decline in the concentration. The peak at the start of the second period is significantly less than that of the first, but is higher in E3 and E4. This is due to the overall balance between the effect of compaction by raindrops on the initial ploughed soil as well as the growth of the deposited layer during the experiments, which reduces its detachment rate, against the growth in rainfall rate, which increases the detachment rate. For E5 → E7, there is a rapid decrease in suspended sediment concentration at the beginning of each period due to the reduction in rainfall intensity. Figure 4 also shows similar suspended sediment concentrations measured at both collectors. At the end of the experiment, the concentrations measured at the collectors 1 and 2 were 1.70 and 2.20 g L^{-1}, respectively.

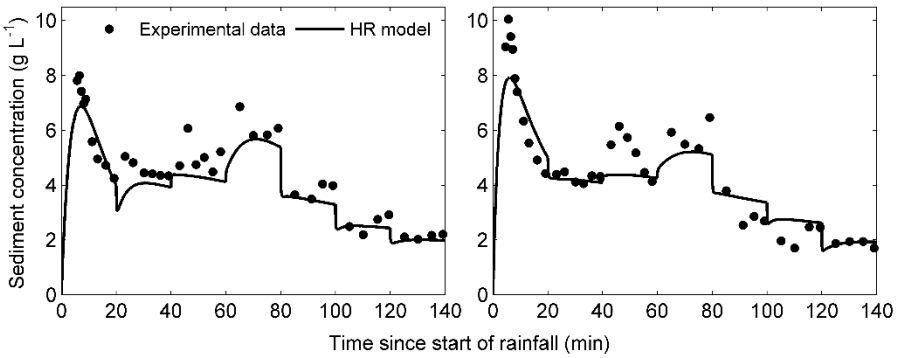

Figure 4. Sediment concentration versus time of the collector 1 (left) and the collector 2 (right).

4.3. HYSTERESIS LOOPS

The maximum sediment concentration occurs before the maximum discharge (Figures 3 and 4) and a clockwise hysteresis pattern results (Figure 5). The experiment started with the soil being initially ploughed, so as mentioned above we began with a soil surface that was easily eroded and led to a high sediment flux and concentration on the rising limb of the discharge hydrograph. During this time, the easily eroded soil was being removed, while simultaneously the surface was undergoing compaction due to raindrop impact. On the falling limb of the hydrograph the deposited layer was much more developed, i.e., had greater mass than on the rising limb, and since this layer is preferentially composed of larger particles, it is also more difficult to erode. Hence for the same discharge, the suspended sediment concentrations were higher on the rising limb than they for the falling limb, and a clockwise hysteresis loop formed.

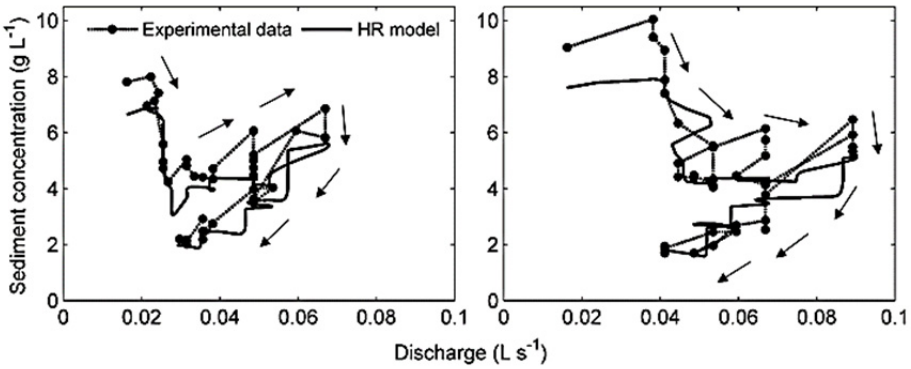

Figure 5. The hysteresis loop generated for collector 1 (left) and collector 2 (right).

4.4. MODEL RESULTS

Estimated HR model parameter values are presented in Table 1. The maximum values of detachability (a) and redetachability (a_d) and the minimum critical mass per unit area to protect the original soil (m^*) were obtained for the initial rainfall period. For subsequent rainfall periods (E2-E7), these values are of largely similar magnitude while they differ from those of the first period (which reflect the initial preparation of the soil). Also, the water depth decreases or increases along with the rainfall intensity. In general, the agreement between the HR model and experiment (Figures 4 and 5) is considered as being satisfactory.

Table 1. Detachability (a), redetachability (a_d), the critical mass of the deposited layer (m^*) and the water layer depth (D) for each rainfall event.

Rainfall Event	Parameter	E1	E2	E3	E4	E5	E6	E7
Collector 1	a (mg cm^{-3})	47	15	13	35	18	15	19
	a_d (mg cm^{-3})	1247	1026	1092	1063	978	937	1175
	m^* (mg cm^{-2})	5.2	23.7	23.4	23.1	31.4	34.1	31.8
	D (mm)	1.4	1.6	14.9	14.9	0.6	0.5	0.4
Collector 2	a (mg cm^{-3})	34	11	13	22	18	18	20
	a_d (mg cm^{-3})	1533	1199	971	958	935	944	951
	m^* (mg cm^{-2})	7.9	32.2	30.3	31.5	34.6	34.9	35.1
	D (mm)	0.5	1.5	14.5	14.8	0.3	0.3	0.1

4.5. DEPOSITED MASS

The HR prediction of the mass of the deposited layer is presented in Figure 6 for both collectors. The degree of shielding (dimensionless) is the ratio of the total deposited mass to the critical mass (m^*), which was defined in section 3. As is evident from Figure 6, regardless of the precipitation rate, the total deposited mass increases continuously during the experiment. On the other hand, there is some variation in the degree of shielding, which stems from the different values of the critical deposited mass (m^*) used for each erosion period (E1-E2) and the sudden changes in rainfall intensity imposed during the experiment. Particularly, in the second rainfall event, there was a sudden decrease in the degree of shielding. In fact, after the first rainfall event, the soil was still undergoing compaction due to the initially low rainfall intensity of 15 mm h^{-1}. When, subsequently, the precipitation rate doubled to 30 mm h^{-1}, there was a marked increase in the erosion of the deposited layer. The high rainfall intensity and incomplete soil compaction resulted in an increased model-estimated critical mass and, therefore, the degree of shielding suddenly decreased (Figure 6).

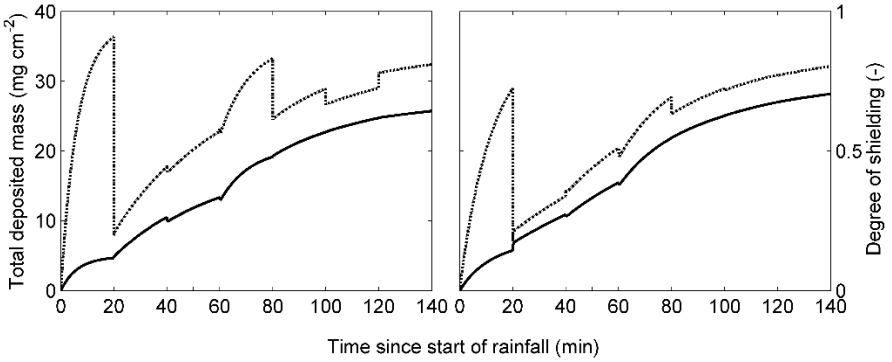

Figure 6. Deposited mass (solid lines) and shield layer development (dashed lines) based on the results of the collector 1 (left) and the collector 2 (right).

5. CONCLUSIONS

Hysteresis effects in splash erosion were investigated by applying seven sequential periods of different precipitation rates in a laboratory flume experiment. The changes in the sediment concentration, shield layer development and hysteresis were analysed. The experimental results show a clockwise hysteresis loop in the sediment concentration versus discharge plot. The physical basis of this loop is the higher availability (due to the prepared, ploughed soil imposed as the initial condition) of sediment in the rising discharge limb relative to lower availability (more compacted and protected soil state) during the falling limb. The Hairsine-Rose (HR) model was validated (via calibration) using the experimental data, which showed its robustness in replicating hysteretic soil erosion delivery under multiple rainfall events.

REFERENCES

1. Baril, P., 1991. Erodibilité des sols et érodabilité des terres : Application au plateau vaudois. Ecole Polytech. Féd. de Lausanne (EPFL), Lausanne, Switzerland.
2. Barry, D. a., Sander, G.C., Jomaa, S., Heng, B.C.P., Parlange, J.-Y., Lisle, I.G., Hogarth, W.L., 2010. Exact solutions of the Hairsine–Rose precipitation-driven erosion model for a uniform grain-sized soil. J. Hydrol. 389, 399–405.
3. Batalla, R.J., Gomez, C.M., Kondolf, G.M., 2004. Reservoir-induced hydrological changes in the Ebro River basin (NE Spain). J. Hydrol. 290, 117–136.
4. Beuselinck, L., Govers, G., Hairsine, P.B., Sander, G.C., Breynaert, M., 2002. The influence of rainfall on sediment transport by overland flow over areas of net deposition. J. Hydrol. 257, 145–163.
5. Gao, B., Walter, M.T., Steenhuis, T.S., Parlange, J.-Y., Nakano, K., Rose, C.W., Hogarth, W.L., 2003. Investigating ponding depth and soil detachability for a mechanistic erosion model using a simple experiment. J. Hydrol. 277, 116–124.
6. Hairsine, P.B., Rose, C.W., 1991. Rainfall Detachment and Deposition: Sediment Thansport in the Absence of Flow-Driven Processes 320–324.

7. Hairsine, P.B., Rose, C.W., 1992. Modeling water erosion due to overland flow using physical principles: 1. Sheet flow. Water Resour. Res. 28, 237–243.
8. Hairsine, P.B., Sander, G.C., Rose, C.W., Parlange, J.Y., Hogarth, W.L., Lisle, I., Rouhipour, H., 1999. Unsteady soil erosion due to rainfall impact: A model of sediment sorting on the hillslope. J. Hydrol. 220, 115–128.
9. Halliday, S.J., Skeffington, R.A., Bowes, M.J., Gozzard, E., Newman, J.R., Loewenthal, M., Palmer-Felgate, E.J., Jarvie, H.P., Wade, A.J., 2014. The water quality of the River Enborne, UK: Observations from high-frequency monitoring in a rural, lowland river system. Water (Switzerland) 6, 150–180.
10. Heilig, a., DeBruyn, D., Walter, M.T., Rose, C.W., Parlange, J.-Y., Steenhuis, T.S., Sander, G.C., Hairsine, P.B., Hogarth, W.L., Walker, L.P., 2001. Testing a mechanistic soil erosion model with a simple experiment. J. Hydrol. 244, 9–16.
11. Jomaa, S., Barry, D. a. a., Brovelli, a., Sander, G.C.C., Parlange, J.-Y.Y., Heng, B.C.P.C.P., Tromp-van Meerveld, H.J.J., 2010. Effect of raindrop splash and transversal width on soil erosion: Laboratory flume experiments and analysis with the Hairsine–Rose model. J. Hydrol. 395, 117–132.
12. Jomaa, S., Barry, D. a., Brovelli, a., Heng, B.C.P., Sander, G.C., Parlange, J.-Y., Rose, C.W., 2012. Rain splash soil erosion estimation in the presence of rock fragments. Catena 92, 38–48.
13. Jomaa, S., Barry, D. a., Heng, B.C.P., Brovelli, a., Sander, G.C., Parlange, J.-Y., 2013. Effect of antecedent conditions and fixed rock fragment coverage on soil erosion dynamics through multiple rainfall events. J. Hydrol. 484, 115–127.
14. Kinnell, P.I.A., 2013. Modeling of the effect of flow depth on sediment discharged by rain-impacted flows from sheet and interrill erosion areas: A review. Hydrol. Process. 27, 2567–2578.
15. Lisle, I.G., Rose, C.W., Hairsine, P.B., Sander, G.C., 1998. Stochastic sediment transport in soil erosion. J. Hydrol. 204, 217–230.
16. Parlange, J.-Y., Hogarth, W.L., Rose, C.W., Sander, G.C., Hairsine, P., Lisle, I., 1999. Addendum to unsteady soil erosion model. J. Hydrol. 217, 149–156.
17. Polyakov, V.., Nearing, M.., 2003. Sediment transport in rill flow under deposition and detachment conditions. Catena 51, 33–43.
18. Sander, G.C., Hairsine, P.B., Rose, C.W., Cassidy, D., Parlange, J., 1996. Unsteady soil erosion model , analytical solutions and comparison with experimental results 178, 351–367.
19. Sander, G.C., Zheng, T., Heng, P., Zhong, Y., Barry, D.A., 2011. Sustainable soil and water resources: modelling soil erosion and its impact on the environment 45–56.
20. Tromp-van Meerveld, H.J., Parlange, J.-Y., Barry, D. a., Tromp, M.F., Sander, G.C., Walter, M.T., Parlange, M.B., 2008. Influence of sediment settling velocity on mechanistic soil erosion modeling. Water Resour. Res. 44, 1–17.
21. Viani, J.-P., 1986. Contribution à l'étude expérimentale de l'érosion hydrique. Ecole Polytechnique Fédérale de Lausanne (EPFL).
22. Walling, D.E., Webb, B.W., 1985. Estimating the discharge of contaminants to coastal waters by rivers: Some cautionary comments. Mar. Pollut. Bull.